MOLECULAR DYNAMICS SIMULATIONS OF MECHANICAL PROPERTIES OF $CU_{70}NI_{30}$ ALLOY

Nguyen Thi Thao(*), Hoang Thi Thu Huong

[1]Hanoi National University of Education

Abstract: *The mechanical properties of polycrystalline $Cu_{70}Ni_{30}$ sample was simulated by Molecular dynamics (MD) simulations. The interaction potential used in the calculations for interactions between atoms in the sample is the Quantum Sutton-Chen embedded potential. This sample at temperature of 300 K consists of the face-centered cubic (fcc), hexagonal closest packed (hcp) structures and few disordered structures. Mechanical properties of this sample was determined by using the uniaxial tensile test. With increasing strain, the crystal structures disintegrate into disordered structures. During deformation process, the number of big simplexes with $R_S \geq 1.95$ Å increase and this process occurs only in the disordered structures. The shear band is formed under the deformation process. The big simplexes form in the shear band and causing the crack propagation.*

Keywords*: CuNi alloys, deformation, simplex, shear band.*

Received 21 November 2021

Revised and accepted for publication 26 January 2022

(*) Email: thaont@hnue.edu.vn

1. INTRODUCTION

Mechanical properties of Cu-Ni alloys have been widely studied both experimentally and theoretically due to the high demand for technology [1-4]. The mechanical characteristics of materials are interested in research such as dislocations, hardness, shear strain, plastic and elastic deformation [3-4]. The mechanical properties of Cu-Ni alloys depend on the method of fabrication, the temperature, pressure, and concentration of atoms. The atoms region with high shear strain of the deposited Cu-Ni film on Ni substrate increases as rising the Cu contents in the Cu_xNi_{100-x} alloy composition [3]. The increase of the Ni concentration in Cu-Ni alloy reduces the threshold value of the indentation depth, at which structural defects begin to generate in the material [4]. The stacking fault energies, yield strength and ultimate tensile strength of Cu-Ni alloys increases with increasing Ni content [1, 5-6]. Actually, the mechanical properties such as Young's modulus, hardness, wear resistance or resistance to plastic deformation can be improved by varying the deposit. For

nanocystaline Cu, plastic deformation is generally dominated by dislocation propagation inside crystals rather than grain boundary siding [7]. During the tensile test, an interfacial void causes dislocations and crack nucleation at the void. Bilayer films with a larger void have earlier nucleation and propagation of dislocations from the void [8]. However, the evolution and distribution of large voids during tensile strain on CuNi alloys have not been investigate yet.

The present work investigates the deformation and mechanical properties of polycrystalline $Cu_{70}Ni_{30}$ alloy sample. The common neighbor analysis (CNA) was used to analyze the microstructure change of these polycrystalline structures during tensile loading [9]. The microstructure, changed during the tensile loading. The clusters of big simplexes were determined to detect the crack propagation at the large strain.

2. CONTENT

2.1. Computational Methods

The sample of $Cu_{70}Ni_{30}$ alloy has the size of 8788 atoms (6151 Cu and 2637 Ni atoms). The quantum Sutton-Chen (Q-SC) embedded potential was used for atomic interactions [10]. Sample was heated at 2000 K at the pressure of 0 GPa for 100 ps to break the original random structure. Then this sample was cooled down to 1200 K at the cooling rate of $4x10^{12}$ K/ps, and cooled down to 300 K at the cooling rate of 10^{12} K/ps. The RDF was calculated to determine the local structure of samples. The coordination number of atoms was calculated based on the use of the cut-off radius as the first minimum of the pair radial distribution function (RDF). The CNA was used to determine structure of atoms [11].

The tensile deformations was carried out on these samples at temperature of 300 K. The detail information of method was described in detail elsewhere [12]. These samples were stretched along z- axis. To evaluate the porosity of samples, we used the simplex analysis, which was presented in detail elsewhere [13]. We known that four atoms of the simplex form a cage around a spherical void. In this sample, the simplexes consist of Cu and Ni atoms, which define as Cu-Ni simplexes, and the simplexes contain only Cu atoms or only Ni atoms, which define as Cu simplexes or Ni simplexes, respectively. We analyzed the development of simplexes existing in these samples during the deformation process. Especially, we have focused on the simplexes with the radius, R_S, larger than 1.95 Å to evaluate the crack propagation in these samples.

To evaluate the plastic deformation at the atomic level under the tensile deformation, the atomic local shear strain η_i^{Mises} was calculated as follows [14]:

$$\eta_i^{Mises} = \sqrt{\eta_{xy}^2 + \eta_{yz}^2 + \eta_{zx}^2 + \frac{\left(\left[\eta_{xx-}\eta_{yy}\right]^2 + \left[\eta_{yy-}\eta_{zz}\right]^2 + \left[\eta_{zz-}\eta_{xx}\right]^2\right)}{6}}$$

where η_{xy}, η_{xz}, η_{yz} are the shear components and η_{xx}, η_{yy}, η_{zz} are the normal components of the strain at the atom i.

2.2. Results and discussions

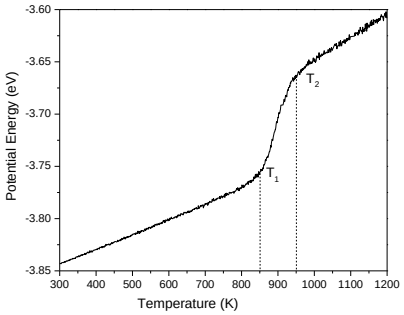

Fig. 1. The potential energy as a function of temperature under cooling process

When the sample of $Cu_{70}Ni_{30}$ alloy was cooled with the cooling process described above, it undergoes a crystalline phase transition. This transition is observed through the potential energy (PE), the number of different types of atoms and the total RDF during cooling process. Fig.1 shows the change of PE of atoms during cooling process from 1200 K to 300 K. As shown in Fig.1, the temperature range of phase transition is at 850 K-950 K at which there is a sudden change of PE of atoms. This result is also shown in Fig.2 and Fig.3. The CNA analyses the structure of the sample as presented in Fig.2. The crystalline structures in the sample include fcc and hcp structues, no bcc structure appears. As the temperature decreases, the number of crystalline atoms increases, while the number of atoms with disordered structures decreases. The temperature range of phase transition corresponds to the range of sudden changes of these values. At temperature of 300 K, sample contains 7296 crystal atoms and 1492 atoms with disordered structure. The structure of the sample during cooling process is also shown by total RDF (see Fig.3). At temperature of 300 K, this RDF shows more clear peaks that indicates the ordered structure of this sample.

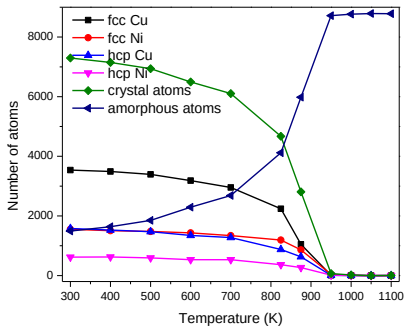

Fig. 2. The number of different types of atoms as a function of temperature under cooling process

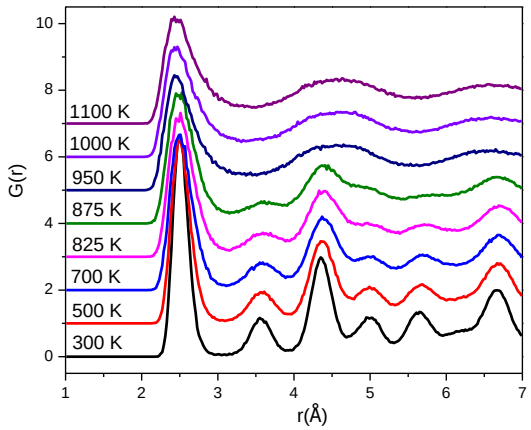

Fig. 3. The total RDF as a function of temperature under cooling process

Fig.4 shows the stress – strain curve of the $Cu_{70}Ni_{30}$ sample during the tensile deformation. According to this curve, the tensile deformation can be divided into three parts: the initial elastic region (ε=0 - 0.044), the elastic-plastic region (ε=0.044-0.165) and the plastic region (ε>0.165). The value of elastic modulus of this sample is 150 GPa. These values are close to the experimental value [15]. After the linear region, the stresses increase with increasing strain in the elastic-plastic region. They reach the ultimate tensile stress of 7.75 GPa. Then it decreases. With further increasing strain, the stress of these samples decrease quickly to zero in the plastic region.

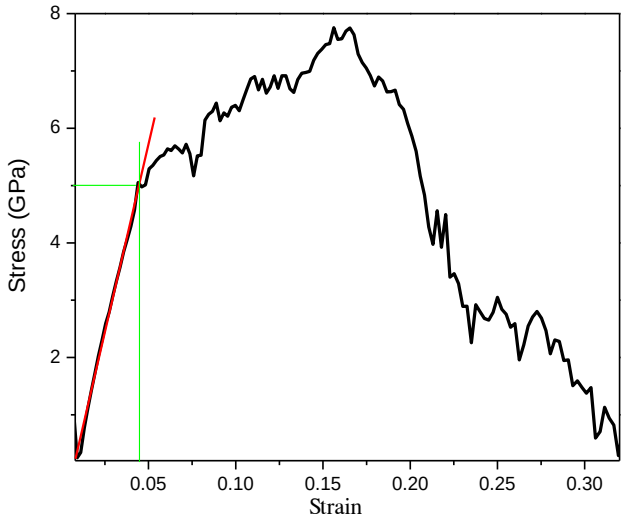

Fig. 4. The stress as a function of the strain under the tensile test at 300 K

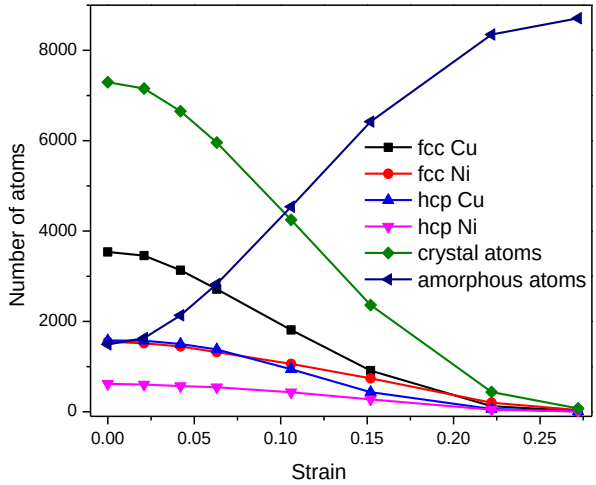

Fig. 5. The variation of the number of different types of atoms under the tensile test at 300 K

Under the tensile test, crystalline Cu and Ni atoms transform into disordered structure (see Fig.5). When the strain is larger than 0.165, structure of atoms in the sample has mainly disordered structure. This means that there are mainly disordered structure in the plastic region.

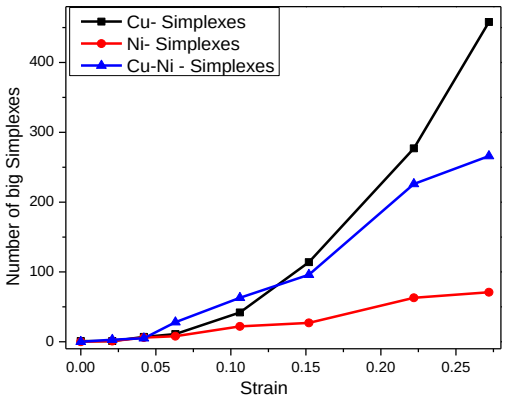

Fig. 6. The number of big simplexes with the radii $R_S \geq 1.95$ Å as a function of the strain

We note that the evolution and coalescence of the big simplexes form the large pores and cause the crack propagation. Here we examined the big simplexes with $R_S \geq 1.95$ Å during the deformation process. Fig. 6 shows the variation of the number of big simplexes, with the radii is larger than 1.95 Å, as a function of strain. One can see that, in the initial elastic region, the number of these big simplexes increases slightly. Then, in the elastic-

plastic and plastic regions, the number of big Ni simplexes increases gradually but ones of big Cu and Cu-Ni simplexes increase quickly with increasing strain. The visualization of big simplexes are presented in Fig. 7. The big simplexes get together to form clusters at the ε=0.063. When the strain increases, these big simplexes gather to form the larger cluster. we can see only one large cluster and a few big simplexes around at the ε=0.106. These clusters increase rapidly in the number of big simplexes with increasing strain. We also determined the largest cluster of big simplexes, which contains the largest number of big simplexes (see in Fig. 6). The result shows that the number of simplexes in the largest cluster increases with increasing strain. At the ε = 0.272, the largest cluster contains 220 big simplexes. We know that, the large pores are formed in the clusters of big simplexes. Therefore, the clustering of big simplexes forms a chain of large pores, at which crack propagation occurs.

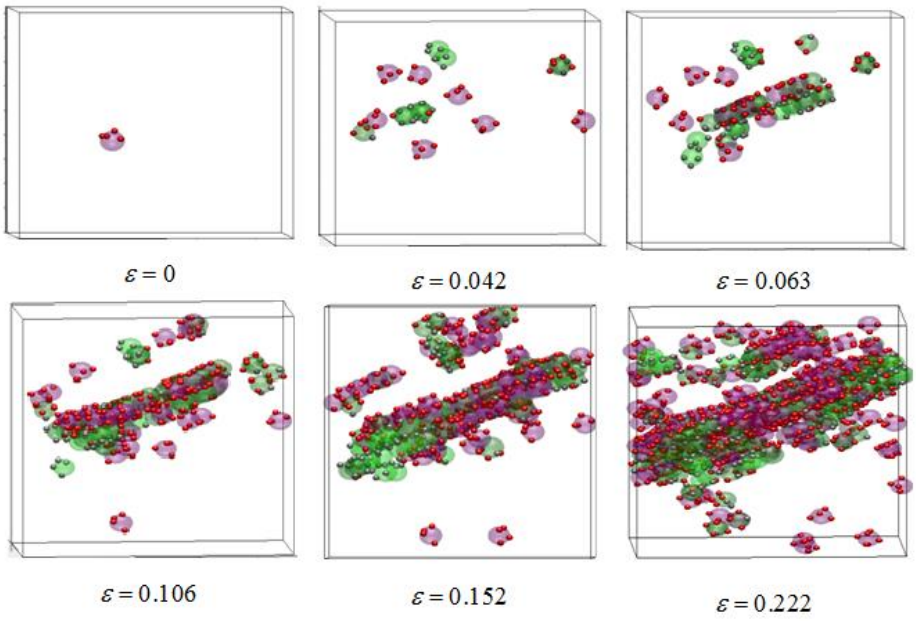

Fig. 7. Visualization of big simplexes, RS ≥ 1.95 Å, with increasing strain (red colour: Cu simplex, green colour: Ni simplex and cian colour: Cu-Ni simplex)

The concentration of plastic strains was analyzed via the atomic local shear strain, η_i^{Mises}. A large value of η_i^{Mises} indicates that atom i undergoes shear deformation, whereas a small one implies that atom i undergoes a small displacement relative to all its neighboring atoms. Fig. 8 shows atoms with the value of η_i^{Mises}, which was calculated with Δε = 0.006 between the current and reference configurations. One can observe that the shear band (SB) propagates at a direction ~45° from the tensile direction. With increasing strain to 0.063, void coalescence begins to occur in SBs. At the higher strain, the crack propagation occurs by void coalescence in SBs.

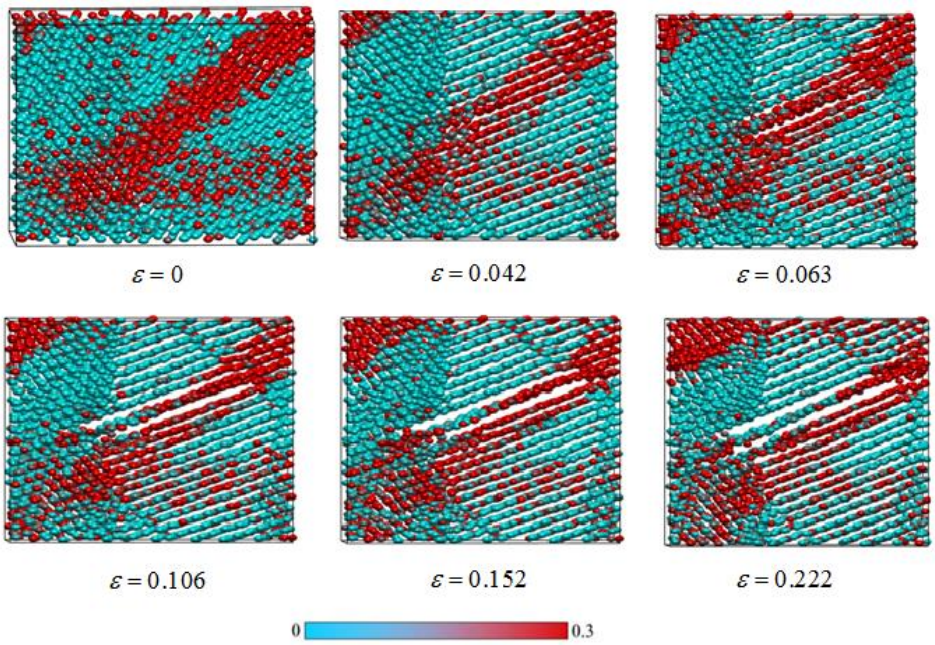

Fig. 8. Atoms are visualized according to their atomic shear strain calculated with Δε = 0.006

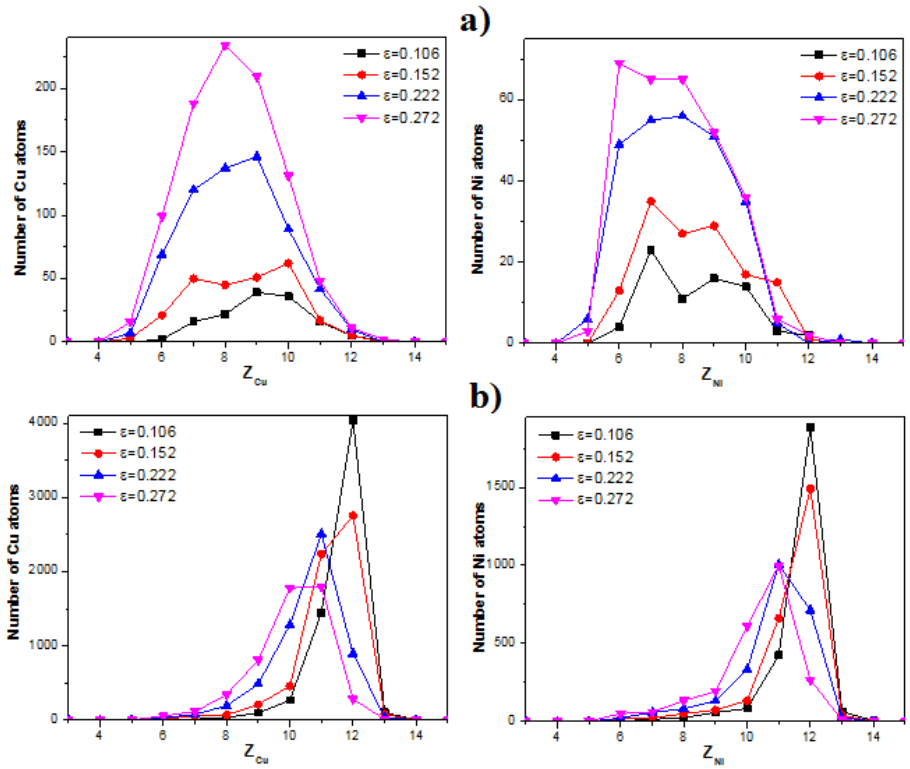

Fig.9. The coordination number (Z) distributions of Cu and Ni atoms at the different strain: a) atoms belong to the big simplexes and b) atoms do not belong to the big simplexes.

Fig. 9 shows the coordination number (Z) distributions of atoms belonging to big simplexes (Fig. 9a) and do not belong to the big simplexes (Fig. 9b). We know that the Z in the fcc and hcp crystals is 12. The atoms with the Z lower than 10 are majority at all of the strains under considerations for the atoms belonging to the big simplexes. Especially, the peak of the Z distribution locates at Z=8 for both Cu and Ni atoms at the strain ε = 0.272. For the atoms do not belong to the big simplexes (see in Fig. 9b), the peak of the Z distribution locates at Z=12 and is sharp at the ε=0.106 and ε=0.152. With further increasing strain, the peak lowers and broadens to the lower Z, indicating that the distances between neighboring atoms are stretched gradually under the tensile deformation.

3. CONCLUSION

Molecular dynamics simulations was performed on $Cu_{70}Ni_{30}$ alloy model with polycrystalline structure. The uniaxial tensile strain carried out on this sample has shown that the deformation process takes place in three stages: the initial elastic deformation, the elastic-plastic deformation and the plastic deformation. As strain increases, the number of crystalline atoms decreases, the number and the size of simplexes increase. The growth of big simplexes with $R_S \geq 1.95$ Å occurs only in disorder structures and in the shear band. The SB continues to propagate with increasing strain. The evolution and coalescence of big simplexes forms a chain of large pores in the SB across the sample, at which crack propagation occurs.

Acknowledgment

This research is funded by the Vietnamese Ministry of Education and Training project (B2020-SPH-01).

REFERENCES

1. WangZY, HanD, LiXW (2017), Competitive effect of stacking fault energy and short-range clustering on the plastic deformation behavior of Cu-Ni alloys. Mater. Sci. Eng. A; 679: 484-492.
2. T. Fu, X. Peng, X. Chen, S. Weng, N. Hu, Q. Li, Z. Wang (2016), Molecular dynamics simulation of nanoindentation on Cu/Ni nanotwinned multilayer films using a spherical indenter, Sci. Rep. 6, 35665
3. Anh-Vu Pham, Te-Hua Fang, Anh-Son Tran, Tao-Hsing Chen (2020); Structural and mechanical characterization of sputtered CuxNi100-x thin film using molecular dynamics; Journal of Physics and Chemistry of Solids 147, 109663.
4. Dmitrii S. Kryzhevich, Aleksandr V. Korchuganov , Konstantin P. Zolnikov, *and* Sergey G. Psakhie (2016), Plastic Deformation Nucleation in Elastically Loaded CuNi Alloy during Nanoindentation; AIP Conference Proceedings 1783, 020121
5. W. Li, S. Lu, Q.M. Hu, K. Kwon, B. Johansson, L. Vitos (2014), Generalized stacking fault energies of alloys, J Phys-Condens. Mat. 26, 277.
6. S. Lu, Q.M. Hu, E.K. Delczeg-Czirjak, B. Johansson, L. Vitos (2012), Determining the minimum grain size in severe plastic deformation process via first-principles calculations, Acta Mater. 60, 4506.

7. H. Zhang, Z. Jiang and Y. Qiang (2009), Microstructure and tensile deformation of nanocrystalline Cu produced by pulse electrodeposition , *Mater. Sci. Eng. A*, 517, 316-320
8. WuCD, HuangBX, LiHX (2020), Effects of interfacial defect on deformation and mechanical properties of Cu/Ni bilayer—A molecular dynamics study, Thin Solid Films; 707: 138050.
9. J.D. Honeycutt, H.C. Andemen (1987), Molecular dynamics study of melting and freezing of small Lennard-Jones clusters, J. Phys. Chem. 91, 4950–4963
10. S.N. Medyanik, S. Shao (2009), Strengthening effects of coherent interfaces in nanoscale metallic bilayers, Comput. Mater. Sci. 45, 1129–1133.
11. FakenD, JonssonH (1994), Systematic analysis of local atomic structure combined with 3D computergraphics. Comput. Mater. Sci.; 2: 279.
12. SchiotzJ, VeggeT, Di TollaFD, JacobsenKW (1999), Atomic-scale simulations of the mechanical deformation of nanocrystalline metals. Phys. Rev. B.; 60: 11971.
13. Le VV, LienLTH (2021). Structural and mechanical properties of densified $(Li_2O)_{0.2}(SiO_2)_{0.8}$ glasses: A molecular dynamics simulations study.J. Non-Cryst. Solids.; 564: 120840.
14. Shimizu F, Ogata S, Li J. (2007), Theory of Shear Banding in Metallic Glasses and Molecular Dynamics Calculations.Mater. Trans.; 48: 2923.
15. T. D. Shen and C. C. Koch, T. Y. Tsui and G. M. Pharr (1995); On the elastic moduli of nanocrystalline Fe, Cu, Ni, and Cu-Ni alloys prepared by mechanical milling/alloying; J. Mater. Res., Vol. 10, No. 11.

MÔ PHỎNG ĐỘNG LỰC HỌC PHÂN TỬ ĐẶC TRƯNG CƠ TÍNH CỦA HỢP KIM $CU_{70}NI_{30}$

Tóm tắt: *Đặc trưng cơ tính của hợp kim $Cu_{70}Ni_{30}$ đa tinh thể được nghiên cứu thông qua mô phỏng động lực học phân tử (MD). Thế tương tác được sử dụng để tính toán các tương tác giữa các nguyên tử trong mẫu là thế tương tác nhúng lượng tử Sutton-Chen. Mẫu hợp kim tại 300 K chứa chủ yếu các nguyên tử với cấu trúc tinh thể lập phương tâm mặt (fcc), lục giác xếp chặt (hcp) và một ít nguyên tử với cấu trúc mất trật tự. Đặc trưng cơ tính của mẫu này được xác định bởi việc sử dụng phương pháp biến dạng đơn trục. Khi biến dạng tăng, cấu trúc tinh thể bị tan rã thành các cấu trúc mất trật tự. Trong quá trình biến dạng, số lượng các simplex lớn với kích thước lớn hơn 1.95 Å tăng và quá trình chỉ xảy ra trong miền cấu trúc mất trật tự. Biến dạng trượt được hình thành trong quá trình biến dạng. Các simplex lớn hình thành trong vùng biến dạng trượt và gây ra sự lan truyền vết nứt trong mẫu.*

Từ khóa: *hợp kim CuNi, biến dạng, simplex, biến dạng trượt.*